
YRiS **Yellow River Studies**

News Letter Vol.4

April 1, 2005

I.	Water Resources Managements in the Fen River Basin	2
II.	Development of a Model for Assessment of Irrigation Management Performance and application to Hetao Irrigation District in the Yellow River basin	8
III.	Land cover classification over the Yellow River domain using satellite data.....	15
IV.	List of related meeting	27

Water Resources Management in the Fen River Basin

Hidefumi IMURA

Graduate School of Environmental Studies
Nagoya University

1. Introduction

While the Yellow River basin is facing a severe shortage of water resources problems, the situation differs vastly from one area to another. It is usually accepted the whole Yellow River basin can be divided into three areas, namely upper, middle, lower river basin. In our study, the middle river basin was divided into the basins of the Yellow River, the mainstream, the Wei River, a tributary, and the Fen River, another tributary (See Fig. 1) for the purpose of analyzing the local situation in more detail. That is to say, Yellow River basin was divided into 5 areas, namely the upper, middle, lower basins of the mainstream, and basins of the Wei River, a tributary and the Fen River, another tributary to conduct a comparative analysis of the relations between natural conditions, socio-economic conditions, etc. and the supply and demand of water resources.

Since the Fen River basin, branching out from the middle river basin is located in semi-arid land, the volume of water as a whole is decisively little. In particular, as a result of the industrialization and urbanization since the 1980s, the shortage of water resources has become more and more serious. Severe shortage of water resources is coupled with water pollution of surface and ground waters due to insufficient flow volume in the rivers. Various water-saving measures are adopted especially in Tai Yuan City, such as reuse of treated sewage water, and great efforts have also been made to solve the problem by transferring water from the mainstream of the Yellow River. Such circumstances are very suggestive in many senses when the problem for the whole of the Yellow River basin is examined. For this reason, the research team of Nagoya University and Tsinghua University conducted a survey on Tai Yuan, the central city in the Fen River basin and its surrounding area in February 2005. The following is our report on the survey.

2. Overview of Fen River Basin and Tai Yuan City

(1) Overview of Fen River basin

The Fen River, one of the major tributaries of the Yellow River, has the second largest scale, next only the Wei River, in terms of the basin area. Furthermore, its basin, 716 km in overall length and 39,400 km² in area, belonging to Shanxi Province, has a size roughly comparable to that of Kyushu, Japan.

(2) Overview of the state of economy and society

About half of the non-agricultural populations, GDP, Gross Industrial Product in the Fen River basin are concentrated in Tai Yuan City, the provincial capital. GDP per capita of Tai Yuan City is around twice as much as that of the whole Fen River basin. In addition, it is the main industrial city in Northwestern China, where industries such as iron and steel, machinery and chemical industry use large amount of coal which produced in this region.

(3) Overview of the water resources

The precipitation averaged over many years is 468.4 mm. The annual volume of water resources per capita is 243 m³, which is extremely small, accounting for 10.6% of the national average and 33.7% of the average of the Yellow River basin. This situation is particularly severe even when compared to that of the entire basin of the Yellow River which is facing a serious water shortage.

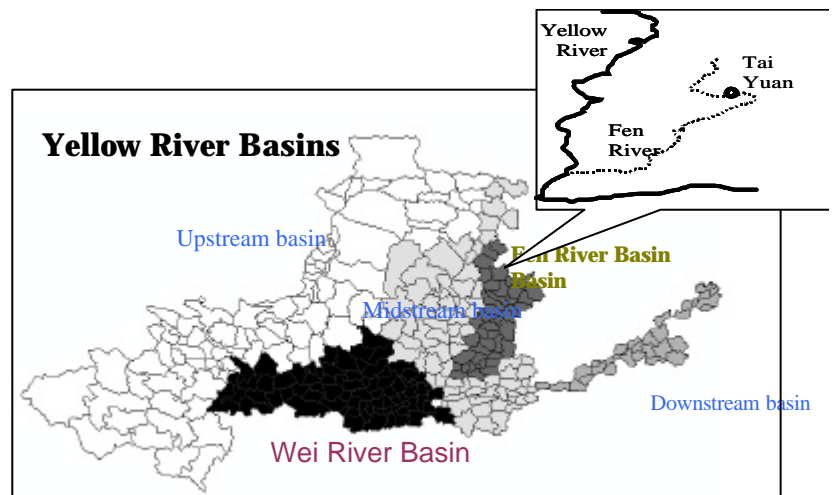


Fig. 1: Segmentation of Yellow River basin and location of Tai Yuan

3. Survey of Tai Yuan City

(1) Items of survey and institutions visited for survey

Our survey was conducted for the objectives stated below:

- To grasp the actual state of water resources and water use in Tai Yuan City.
- To identify trends in the water price under the influence of the Wanjiashai Water Diversion Project.
- To grasp the discharge and treatment of sewage water.
- To understand how the fund for constructing a sewage water treatment plant is collected and how the water price mechanism is established.
- To grasp the water saving policy and the state of reusing of waste water

In order to attain the objectives mentioned above, interviews were conducted at the Taiyuan Environment Protection Bureau, Taiyuan Saving Water Bureau, Taiyuan Water Resources Management Bureau, Taiyuan Municipal Engineering Administration Bureau, Hexi Eizhongbu Sewage Treatment Corporation and Yangjiabao Sewage Treatment Plant. In addition, on-site surveys were conducted at Yangjiabao Sewage Treatment Plant, Hexi Eizhongbu Sewage Treatment Corporation, Nanyan Sewage Treatment Plant, Taiyuan Iron And Steel Company Sewage Treatment Plant (industrial waste water treatment plant) and the Water Saving and Irrigation District Office.

(2) Water resources and water environment



Figure 2: Artificial tourism area on the Fen River (left) Discharge of waste water

The Fen River runs across Tai Yuan City from north to south, though complete desiccation of the surface water in the urban district of Tai Yuan City occurred about 10 years ago. Moreover, domestic waste water is increasing year by year and now exceeds the volume of discharged industrial waste water. On the other hand, although the domestic waste water increases in volume, its treatment rate is less than 50%. As a result, while the Tai Yuan Municipal Government created a pretty artificial tourism area on the Fen River with water stored in the upstream basin, waste water is discharged in the downstream basin.

(3) Wanjiashai Water Diversion Project

The daily life water and industrial water used in Tai Yuan City are dependent mainly on groundwater. The annual volume of groundwater exploitation is 460

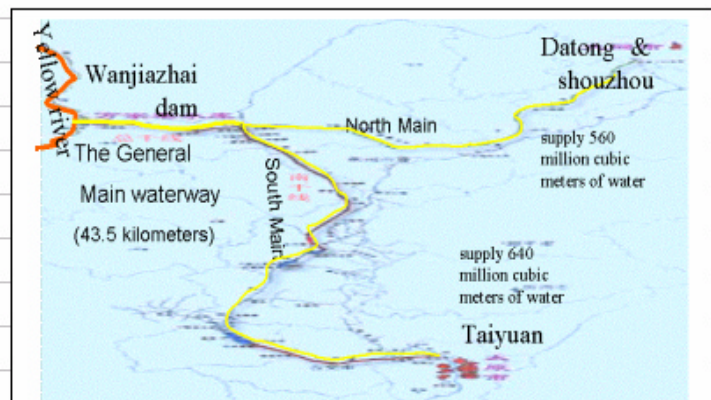


Fig. 3: Wanjiashai Water Diversion Project

Data and Figure source:

<http://www.sxga.com.cn/xiezuodanwei/yinhuang/index.htm>

http://www.tidi.ac.cn/sj/sj_icon/yinhuang/yh_bz_photo/pages/yh_bz1.htm

million m³, and the deepest well in some places has reached a depth of as much as 1,400 meters. The Wanjiashai Water Diversion Project (Fig.3) to introduce water from the mainstream of the Yellow River to the Fen River (“Yellow to Fen Water Introduction”) was proposed and implemented as a drastic measure to overcome such a problem of the shortage of water resources. This project had already begun using water from the Yellow River in October 2003. Our survey revealed that the cost of introducing water from the Yellow River was extremely high, amounting to 8 - 10 Yuan/ ton, placing a heavy burden on both enterprises and households. Moreover, although the Provincial and Municipal Governments are now sharing a part of this cost, a policy has been settled to reduce this sharing gradually in future, which will supposedly increase the burden on households and enterprises further.

(4) Sewage treatment

Attaching enormous importance on the measures to treat sewage, Tai Yuan City constructed the Beijiao Sewage Treatment Plant in 1956. At present, in Taiyuan City, there are 4 municipal sewage treatment plants. They are Beijiao Sewage Treatment Plant (Beijiao), Yangjiabao Sewage Treatment Plant (Yangjiabao), Hexi Beizhongbu Sewage Treatment Corporation (Hexi Bei), and Yangjiabao Sewage Treatment Plant (Yangjiabao). There are 367 sewage pipes linked to these treatment plants with a total length of 340.94 km.

There are 2 industrial sewage treatment plants, namely Taigang Sewage Treatment Plant (Taigang) and the Nanyan Sewage Treatment Plant (Nanyan). (Table 1) (Fig. 1) In addition, there are 2 plants, namely the Chengnan Sewage Treatment Plant and the Jiancaoping Sewage Treatment Plant, are planned to be



Figure 4: Tour of a sewage treatment plant: Yangjiabao Sewage Treatment Plant (left) Hexi Eizhongbu Sewage Treatment Corporation (right)

constructed in the future. Their treatment capacities are 260,000 and 50,000 m³/ day respectively. After put into operation, the ratio of sewage treatment in Taiyuan City is expected to reach 70%.

Table 1: State of sewage treatment plants

	Area for collection of sewage km ²	Designed capacity 10 thousand tons / day	Population benefited by the treatment 10 thousand persons	Volume of sewage treated 10 thousand tons / year	Cumulative investment 10 thousand Yuan	Operation cost Yuan / ton
Municipal sewage treatment plants						
Yangjiabao	58	16.64	56	5353	14253	0.35
Beijiao	18.09	8	16	363	7668.3	1.28
Yinjiabao	21	1	13	375	467	0.84
Hexi Bei	35	15	70	2182	12272	0.36
Industrial sewage treatment plants						
Taigang	-	16.4	-	3650	17000	0.58
Nanyan	-	6	-	1460	5050	-

Placed in order on the basis of the Tai Yuan survey result

(5) Water saving

a) Policy

On the basis of the policy determined by the “Water Law” of the People’s Republic of China and the “Water Resource Management Institute” of Shanxi Province, the Tai Yuan Municipal Government established the “Water Saving Regulation of Tai Yuan City.” According to this regulation, the water saving standard is stricter than the national standard, in consideration of the condition of water resources in Tai Yuan City.

b) Measures

For enterprises:

- The regulatory system for the volume of water for use is to be adopted.
- Where water is used in excess, a water fee 2 ~ 5 times higher than the usual fee is to be charged.
- Industries requiring large water consumption will not be developed.
- In addition, a new enterprise is investigated in advance from the perspective of environmental management.

For households:

- To encourage water saving.
- To encourage the use of water-saving-type equipment in particular.

For agriculture:

- To establish model water-saving irrigation districts. (Fig. 5)
- To promote water-saving irrigation techniques further.
- To build up a system to purchase water for agriculture, using a cash card.
- To control the volume of agricultural water, taking into consideration the water resources conditions and type of agricultural products of each year.

Tai Yuan City has been developing water saving projects since 1980, and the water saving effect is improving, supported by the water pricing policy and administrative regulation. For this reason, it is nationally recognized as one of the water-saving cities.



Figure 5: Model water saving district (left); Cash card apparatus (upper right) Embedded type irrigation pipe (lower right).

Note) This is a system in which a farm household can purchase water, using a cash card under the control of the total volume effected by the government, taking into consideration the volume of water resources and condition of the cultivation of agricultural products of each year.

4. Conclusions

In the Yellow River basin, it is necessary to construct a sustainable society based on a thorough management of water resources. In our survey, we keenly felt that the depletion of water resources in the Fen River basin is a miniature version of the entire Yellow River basin where the same type of problems may arise in a much larger scale, and experiences in the Fen River basin provides valuable suggestions and

insights for formulating future policy measures against water shortage problems in regions placed under similar conditions. We are convinced that the study of the steps taken by Tai Yuan City and investigation of the causes of water resource depletion will lead to the sustainable management of water resources in the entire Yellow River basin.

Based on this survey, we plan to continue studies on the following questions:

- Quantification of the environmental capacity of the Fen River basin in terms of water resources availability and water pollution control
- Allocation schemes of water resources to different sectors
- User fees and cost recovery of water transfer projects such as Wanjiashai Project
- Technological potential of water saving and reuse of treated waste water in industry, agriculture and household sectors

Development of a Model for Assessment of Irrigation Management Performance and application to Hetao Irrigation District in the Yellow River basin

Keisuke HOSHIKAWA, Takanori NAGANO, Takashi KUME, Tsugihiko WATANABE

Research Institute for Humanity and Nature

1. Introduction

IMPAM (Irrigation Management Performance Assessment Model) is a model that is being developed by the authors to simulate water movement and calculate water balance in irrigation areas. IMPAM can be a tool for the assessment of management performance procedures in irrigation areas which strongly affects water balance of in irrigated areas, as well as it can provide important information for simulations of river runoff basin and regional climate.

In addition, IMPAM can simulate water balance after change in water management. Water conservation is one of the most important current concerns in managing irrigation areas throughout the world, and several trials to improve irrigation performance through modification of water management (both physically and operationally) are being pursued. However, changing water management practices can cause unexpected changes in water balances and often bring unintended side effects. For example, modification of a channel system to reduce seepage may produce a drop in groundwater levels, disadvantaging farmers who depend on groundwater (Roost, 2002). It is important therefore to have techniques to predict changes in water balance caused by changes in irrigation management procedures, as well as to assess the present water balance of an irrigated area, to look for problems and suggest how they can be ameliorated.

2. Development of IMPAM

2.1 Scope of IMPAM

To assess and compare water management procedures, the appropriate scale of operation for study would appear to be that which covers the system from farm-block to irrigation district, as the effects of different water management procedures should appear most clearly at this scale; accordingly, this is the scale at which the IMPAM system has been designed to operate. Several earlier water balance models have been developed, but their scales are either too wide or too narrow to describe the effects of management changes on the water balance. Thus, the PODIUM (IWMI, 2000) model simulates the balance of demand and supply at scales ranging from regions to whole countries, and take into consideration socio-economic factors as well as agriculture. The scope of these models is too large; detailed hydrological processes are ignored, and they are therefore not suited to the assessment of irrigation management procedures. On the other hand, models like SWAP and HYDRUS include very precise calculation of the one-dimensional water balance in a farm plot, considering physical aspects of soil water movement. For an irrigation district the water balance often depends more on the physical characteristics of the irrigation system, its operation rules, the cropping pattern and distribution of land use practices etc., than on the water balance of individual farm plots. For example, the water balances of irrigation districts in the Ningxia Autonomous Region (Weining and Qingtongxia IDs) and Hetao ID (Inner-Mongolia Autonomous Region) in the Yellow River basin (Figure 1), China, are quite different, especially in the ratio of drain water to intake water (Figure 2 (a) and (b)). Such difference should be mainly because of differences in the characteristics of these irrigation districts such as operational procedures, physical structures, etc., which cannot be described by one-dimensional water balance models. However, these important components of the water balance of irrigated areas are included in the IMPAM system.

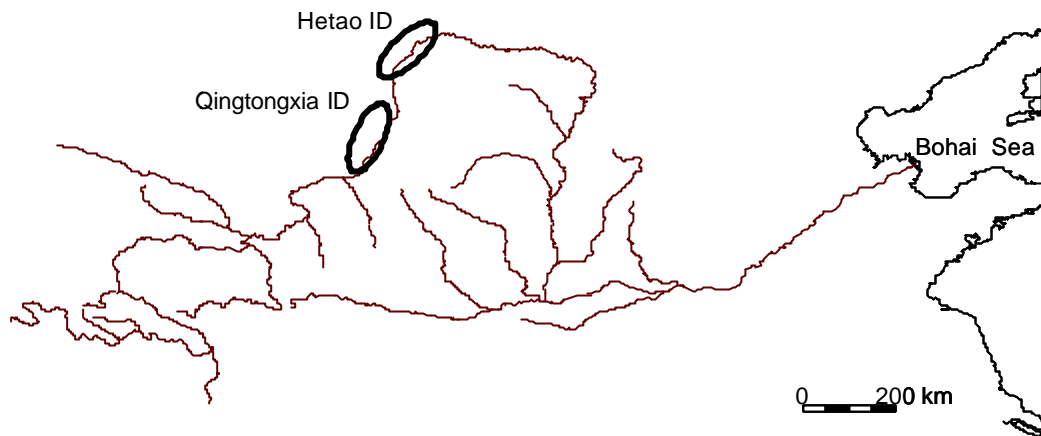


Figure 1. Hetao and Qingtongxia Irrigation Districts

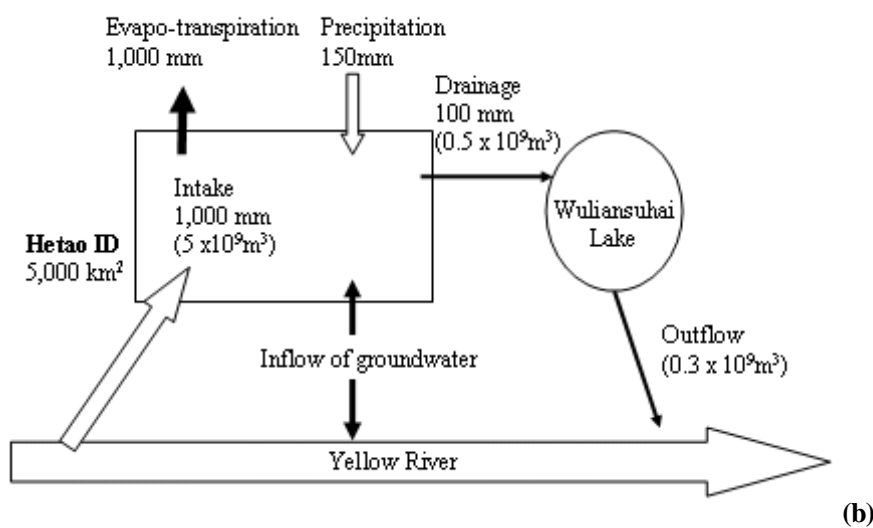
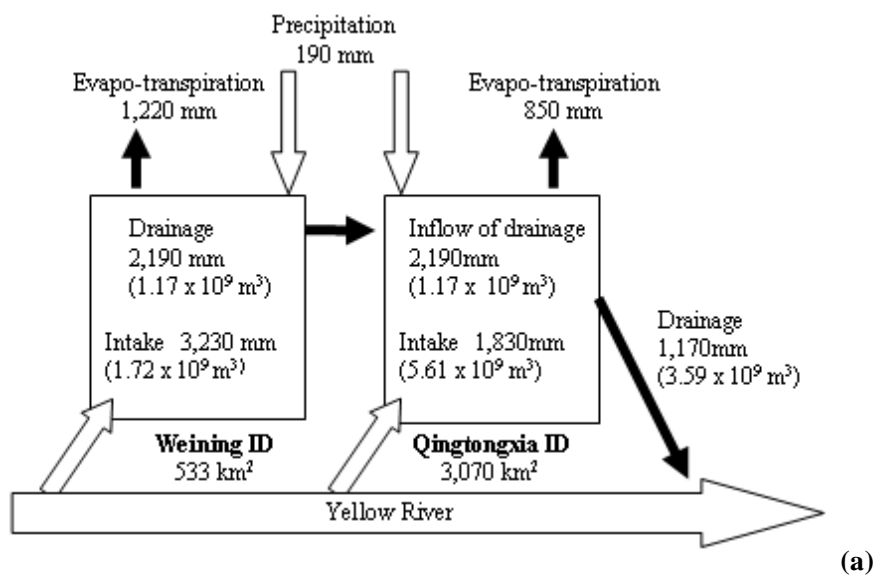


Figure 2. Water balance of Irrigation Districts in Ningxia (a) and the Hetao Irrigation District (b)

2.2 Structure of IMPAM

Use of IMPAM for simulations of water balance, including the district-scale components described above, requires several kinds of dataset, as indicated in Figure 3. IMPAM combines four modules (Water Distribution Module (WDM), Drainage Reuse Module, Spatial Water Balance Module (SWM), and Farm Water Balance Module (FWM)) (Figure 4), to simulate complicated water dynamics in irrigated areas.

The functions of the four modules are as described below.

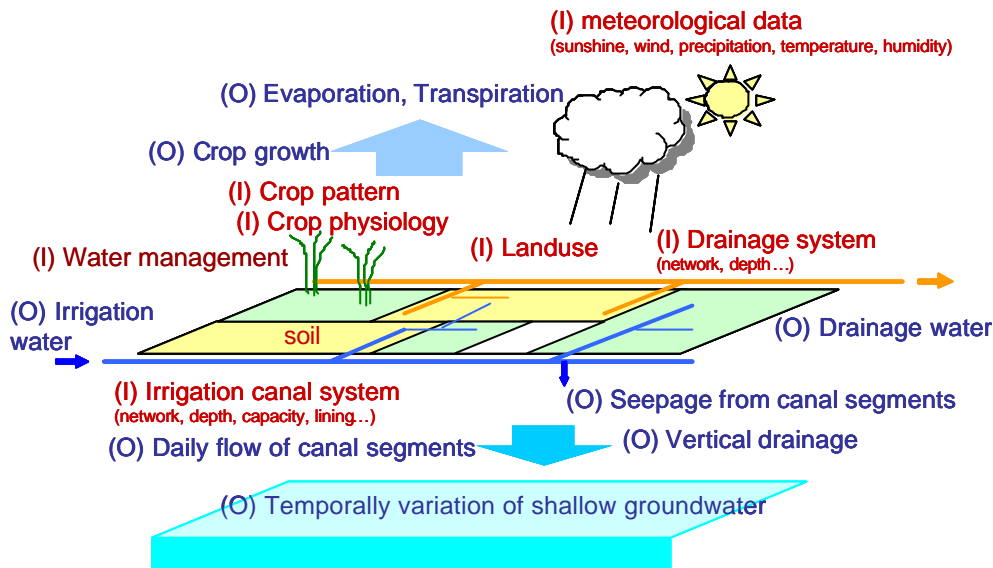


Figure 3. Input (I) and output (O) of IMPAM (Entrée (I) et rendement (O) d'IMPAM)

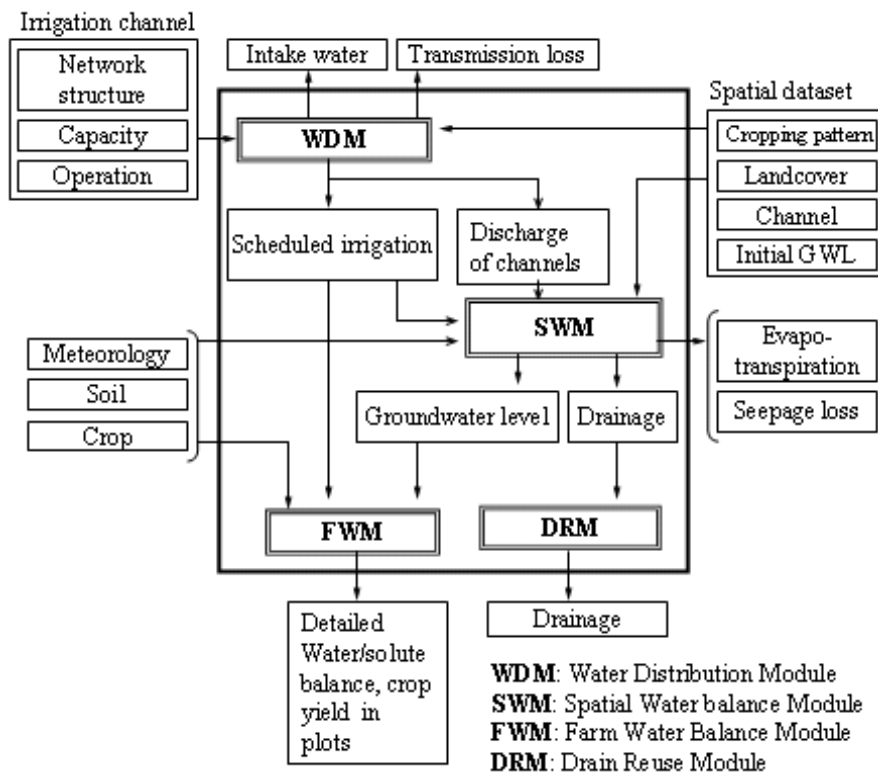


Figure 4. Framework of IMPAM

A. Water Distribution Module

The WDM calculates the daily discharge rate (m^3/s) of each irrigation channel segment, taking into account the amount of seepage loss. The main input items to this module are (i) the topological structure of the irrigation channel network, (ii) the capacity and loss rate of each channel segment, (iii) the date and amount of irrigation for each farm plot and (iv) the crop pattern, and dates of sowing and harvest. Details of dates and amounts of irrigation inputs are derived from reference tables prepared by local government, or can be calculated by the FWM (see below). If the calculated daily discharge supplied is clearly in error (for example, if calculated discharge exceeds channel capacity), channel daily discharge is calculated again after the irrigation schedules have been adjusted.

B. Drain Reuse Module (DRM)

The DRM calculates the total amount of drainage-water from an irrigated area. The layout of the drainage channel network, amount of drainage and amount of reuse of drainage-water of each plot are the main input items to this module.

C. Spatial Water balance Module

The SWM is a quasi-three-dimensional water balance model that calculates the temporal and spatial variation of groundwater levels. Vertical movement of soil moisture in unsaturated zone is governed by Richards equation and horizontal water flow in saturated zone is governed by a differential equation in this module. Meteorology, irrigation schedule, landuse-crop spatial distribution, and the irrigation-drainage channel spatial distribution database are the main input items of this module. This module takes into account evapotranspiration from land areas that are uncropped (such as saline land) and the seepage loss from irrigation channels as factors that affect the water balance. The spatial distribution of seepage from channels is calculated using the channel daily discharge calculated by the WDM. Temporal and spatial variation of groundwater levels is used by the FWM as a lower boundary condition.

D. Farm Water balance Module

The FWM calculates the water balance of each plot (whether bare or fallow) with data inputs such as irrigation schedule, meteorology, crop calendar, soil character parameters, etc. An earlier vertical one-dimensional water balance must be incorporated into this module. In a test application described below, SWAP (Soil Water Atmosphere Plant) was used. Other models, as determined by data availability, can be used to provide the required simulation precision.

3. Application of IMPAM

Applying IMPAM to a lower part of a particular administration area of the Xile secondary channel (Figure 5), Yongji-Irrigation-District in the Hetao Irrigation area, and we simulated water balance changes under three simplified conditions: first, no channel is lined, second, tertiary channels are lined, and third, all channels are lined and no seepage from channel occurs in the area.

In the study area, two tertiary channels (Xile and Nanqu) and 59 quaternary-level channels were included (**Photo 1**) It is estimated that 60% of total water intake to the district is lost as seepage from irrigation channels. The physical structure of the channel system, the frequency and amount of irrigation, the irrigated crop area in the administration area and the water intake periods suggest that the Yongji-Irrigation-District abstracts water on the assumption that about 40% of the total intake will be lost in transmission. We assumed that the ratio of seepage loss to total water intake into the simulation area is about 30%, and in addition, that the loss rate per unit channel length is the same for all channel segments. Using the WDM, we estimated the loss rate per unit channel length to be $6.0 \times 10^{-5} \text{m}^3/\text{m}/\text{s}$, and then developed an assumed rotation pattern.

In the Hetao Irrigation District, irrigation is applied four to five times a year from May to October. The last irrigation is applied after the harvest at the end of September or the beginning of October, for the following year's crop, as water demand in spring is so high that sufficient water cannot be taken from the Yellow River.

Land cover was separated into two classes, cropland and non-cropland, on the basis of optical examination of ASTER satellite images (Figure 6). According to the Yongji-Irrigation-District Management Office (2002), cropland occupies about 72%, close to the result from satellite image classification. To

simplify the simulations, it was assumed that the remaining 28% of the area was bare soil. Corn, wheat and sunflower are mainly cultivated in this irrigation district (**Photo 2**).

The period covered by the simulation was from April 21 to October 31 (194 days), and the area was segmented into 500 x 500-m grids for simulation with the SWM.

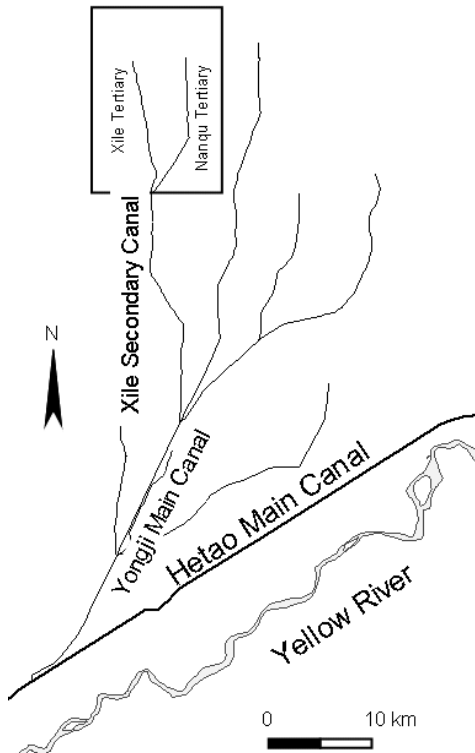


Figure 5. Simulation area

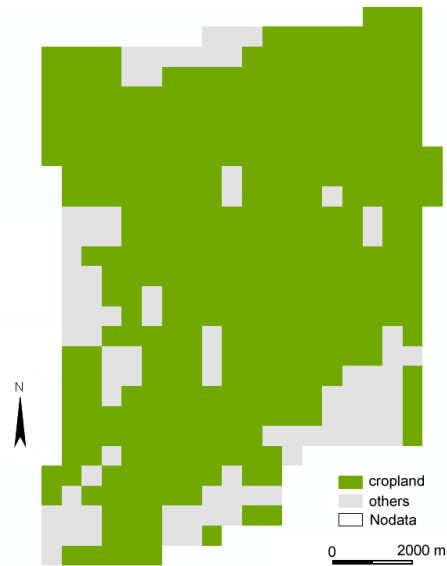


Figure 6. Land cover in the simulation area



Photo 2 Water gate on Yongji Main Canal from which Xile Secondary Canal takes off



Photo 1 Farmland in Yongji Irrigation District.

Simulation 1: Assuming 30% of total water intake is lost as seepage

In simulation 1, it is assumed that no channel is lined and 30% of intake water is infiltrates from channels into subsurface. This assumption about channel seepage is most close to an actual situation.

At the end of the simulation period, groundwater levels along the secondary and tertiary channels were found to be much higher than at the beginning (Figure 8), and waterlogging probably would have occurred in some areas. This suggests that the amount of water applied along the major channels should be reduced relative to other areas.

The fact that a large decline in groundwater level was seen mostly in uncropped areas (**Figure 6 and 7**) indicates that even in situations with soils of high hydraulic conductivity (2.5×10^{-6} m/s in the simulation area), horizontal water flow from irrigated cropland to neighboring non-irrigated land cannot be detected clearly in simulations if the horizontal spatial resolution is in the range of hundreds of meters.

Simulation 2: the secondary channels have no seepage loss

IMPAM-SWM was run assuming that the secondary and tertiary channels were completely lined, with a seepage rate of zero, and also assuming that the seepage rate from the tertiary channels was the same as in the first simulation (6.0×10^{-5} m³/m/s). The conditions for simulation 2 were the same as for simulation 1, except for differences in the loss rates of the tertiary channels. Though a decrease of transmission loss would permit a reduction in the period of rotation of irrigation, the same rotation pattern was used in simulations 1, 2 and 3 in order to evaluate the impact of physical changes in the channel system clearly.

This simulation suggested that lining secondary and tertiary channels might not produce a drastic change in the water balance (**Figures 7 and 8**). In the simulation area, seepage loss seems to occur mostly in the quaternary-level channels because of the rotation pattern. Amount of seepage loss depends on both time and length. As the capacity of each quaternary-level channel is limited, it takes a long time to distribute water to the entire irrigation area. Tertiary channels have water longer hours however total length of tertiary channels is much less than that of quaternary channels in this area. This fact suggests that capacity of quaternary channels should be increased or quaternary channels should be lined to decrease seepage losses effectively.

Simulation 3: no channel seepage loss

When we assumed that all secondary, tertiary and quaternary-level channels were completely lined and that no seepage occurs, the groundwater level was lower at the end of the simulation than at the beginning throughout the simulation area (**Figure 9**), and evapotranspiration was much less than in the case of simulations 1 and 2 (**Table 2**). To avoid reduction in crop yield from water stress, more irrigation water would have to be applied. This result suggests that reducing seepage loss may not always decrease the water intake for irrigation.

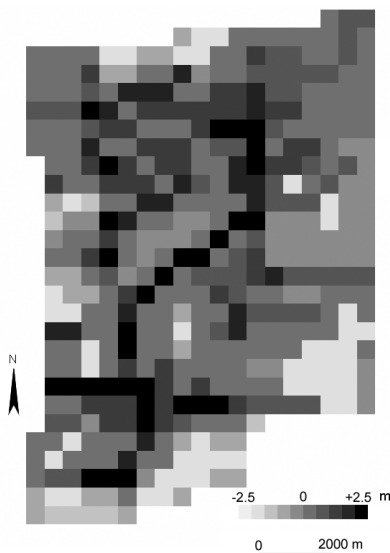


Figure 7. Changes in groundwater level (GWL) (GWL begin – GWL end) (no channel lining)

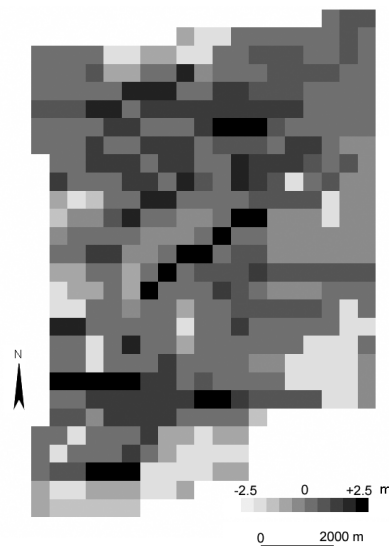


Figure 8. Changes in GWL (GWL begin – GWL end) (with lined secondary and tertiary channels)

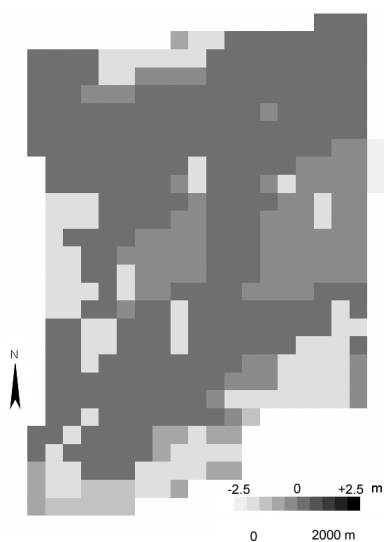


Figure 9. Changes in GWL (GWL begin – GWL end)

Table 2. Total evapotranspiration during the simulation period, averaged over the simulation area (mm)

	Simulation 1	Simulation 2	Simulation 3
Canal conditions	No lining	Secondary and tertiary channels lined	All channels lined
ET (mm)	719	713	688

4. Conclusions

As shown in this paper, IMPAM can be used to estimate water balances under current management practices, and to simulate changes that would result from a proposed change in system management. IMPAM should be a useful tool for evaluating current irrigation management, and for considering how it should be modified. Now development of IMPAM is in progress. Calibration with observed data and information from management offices would improve this model.

Construction of a dam upstream on the Yellow River or modification of the channel system in the Hetao Irrigation District may change the peak of irrigation from autumn to spring. IMPAM can simulate water balance changes resulting from such changes in irrigation management.

References

Akai T., Morimoto K., Shi H. and Li Y., 2004: Methods for improvement of salinity affected land and movement of soil moisture and solute at the on-farm level, *Progress of desertification in cold-arid Asia, recovery of agricultural land and grassland and measures against poverty* (in Japanese and Chinese)

IWMI (International Water Management Institute) 2000. World Water Supply and Demand: 1995 to 2025

Kong D., 2004: Study on crop responses to soil-water salt and its modelling for saline soil under water-saving irrigation, doctoral thesis of Inner-Mongolia Agricultural University, China (in Chinese)

Roost, N., 2002: Improving irrigation water use efficiency, productivity and equity: simulation experiments in the downstream Yellow River basin. *Proc. of 1st International Yellow River Forum on River Basin Management*

Yongji-Irrigation-District Management Office, China, 2002: Yongji Irrigated Area (in Chinese)

Land cover classification over the Yellow River domain using satellite data

Masayuki Matsuoka^a, Tadahiro Hayasaka^a, Yoshihiro Fukushima^a, Yoshiaki Honda^b

^a Research Institute for Humanity and Nature

^b Center for Environmental Remote Sensing, Chiba University

Abstract

Land cover classification is implemented in the East Asian region using 250 m MODIS land surface reflectance product in combination with MODIS snow cover product and OLS human settlements product. This classification map is used as one of the input data of hydrological model applied to the Yellow River in China. The classification method is based on the decision tree classification by means of 11 kinds of land surface features derived from time series of two MODIS products and OLS data in 2000. The province based comparison of classification result with Chinese digital land cover map shows the good agreements in forest, agricultural field, grassland and barren categories. Another comparison with Chinese census results in the slight overestimations in forest and agricultural field. Agricultural sub-categories as paddy, dry field, and irrigated field shows relatively low agreements in both comparisons.

Keywords: Land cover; Decision tree classification; East Asia; MODIS products; OLS product

1. Introduction

Land cover classification over large area by means of remote sensing plays an important role not only in thematic mapping but also in geophysical modeling. Land cover is one of the critical parameters of the hydrological, biophysical, and climatological models to parameterize the geophysical, biological and ecological characteristics of land surface.

The purpose of this study is to create the land cover map of East Asia at the spatial resolution of 7.5 arc seconds using 250 m MODIS land surface reflectance product. Another two satellite derived products, 500 m resolution MODIS snow cover product and 1 km resolution DMSP (Defense Meteorological Satellite Program) human

settlements product are used as auxiliary data to add the separability to some land cover categories. The primary application of this land cover map is hydrological modeling on the Yellow River in China. The Yellow River had been dried up and river water had not been reached to the Bohai Sea for many days in a year since 1970s. Since the main reasons of dry-up are the decrease of precipitation in upstream and excess water use mainly in agriculture, hydrological model, which can deal with the human activity such as water storage and irrigation as well as natural dynamics of water, has been developed based on the SVAT (Soil-vegetation-atmosphere transfer) scheme for the water management (Ma et al., 1998; Ma et al, 2000; Ma et al, 2002). Higher spatial resolution

data of 250 m observed by MODIS is suitable for our purpose because the land cover of East Asia including the Yellow River basin is heterogeneous and it consist of small patches of land cover components such as forests, grasslands, agricultural fields etc. The land cover classification map derived in this study is used as the input data of this hydrological model to capture the area and distribution of land cover elements in the river domain.

2. Methods

2.1 Data

The three kinds of data were used for our classification. Two of them are "MODIS/Terra Surface Reflectance 8-Day L3 Global 250m SIN Grid version 4 (abbreviated as MOD09Q1)" and "MODIS/Terra Snow Cover 8-Day L3 Global 500m SIN Grid version 4 (MOD10A2)". MODIS has been operated since 1999 in order to provide global and long-term respective survey of the Earth (Salomonson et al., 1989) with 36 spectral bands allocated between 0.405 and 14.385 μ m. Third data is "Human Settlements data" included in the product "Nighttime Lights of the World - Change Pair" produced from nighttime brightness observed by OLS (Operational Linescan System) onboard DMSP.

Two MODIS products were acquired through the internet from EOS Data Gateway website (<http://edcimswww.cr.usgs.gov/pub/imswelcome/>). Although the target year of the classification is in 2000, 45 periods of MOD09Q1 and MOD10A2 from 26 February, 2000 to 18 February, 2001 except 12 August, 2000 are utilized for the classification because both data for the period

from 1 January to 18 February in 2000 and MOD10A2 in 12 August were not available. These data are composite data constructed from 8 daily products for minimizing the cloud contamination, therefore the notation of "1 January" correspond to the data from 1 to 8 January. All periods of data were reprojected to Equirectangular (latitude/longitude) projection with the geographical coverage from 20 degree north to 50 degree north in latitude, and 90 degree east to 150 degree east in longitude by MODIS reprojection tool (<http://edcdaac.usgs.gov/landdaac/tools/modis/index.asp>). While original resolutions are 250 m and 500 m, the spatial resolution of reprojected MOD09Q1 is in 7.5 arc seconds and reprojected MOD10A2 is in 15 arc seconds, which correspond approximately to 230 m and 460 m at equator respectively. Human settlements data in 2000 was downloaded from DMSP site (<http://dmsp.ngdc.noaa.gov/dmsp.html>). Since the data is in Equirectangular projection with 30 arc seconds resolution, we just clipped the corresponding area.

2.2 Derivation of land surface features

The following eleven kinds of land surface features were derived as the input metrics of the classification:

1. Ann_Max_NDVI: Annual maximum NDVI.
2. Ann_Min_NDVI: Annual minimum NDVI.
3. Ann_Max_Ref1: Annual maximum band 1 reflectance.
4. Ann_Min_Ref1: Annual minimum band 1 reflectance.
5. Ann_Ave_Ref1: Annual average of band 1

- reflectance.
6. Ann_Max_Ref2: Annual maximum band 2 reflectance.
 7. Ann_Min_Ref2: Annual minimum band 2 reflectance.
 8. Apr_Ave_NDVI: Monthly average of NDVI in April.
 9. Jun_Ave_NDVI: Monthly average of NDVI in June.
 10. Sum_Day_Snow: Number of snow days in summer.
 11. Hum_Set_DMSP: DMSP Human settlements data.

The smoothed time series were derived by moving average of original NDVI (or reflectance) with the temporal window of seven periods in order to avoid the errors and unreasonable fluctuations. The annual maximum and minimum of NDVI and reflectance were selected from this smoothed time series. Since cloud and/or snow were found in some period and in some area, these undesirable data were excluded from sample of moving average by means of quality control flag included in MOD09Q1 and Maximum_Snow_Extent data in MOD10A2.

The Ann_Ave_Ref1 was derived by averaging of the samples from second maximum to second minimum reflectance among the cloud free and snow free reflectance, because maximum and minimum reflectance were excluded in order to avoid erroneous data. Apr_Ave_NDVI and Jun_Ave_NDVI were normal averages derived from cloud free reflectance in 4 periods of data from 6 April to 30 April and from 24 May to 17 June, respectively. Sum_Day_Snow was the number of snow days in summer season derived from Eight_Day_Snow_Cover data included in MOD10A2 product. Snow bits were accumulated through 11 periods of data from 3 July to 29

September. Since the human settlements data is the averaged value of the year, no process but clipping was applied for Hum_Set_DMSP data.

2.3 Land cover categories

We embraced the IGBP (International Geosphere-Biosphere Programme) scheme as basic land cover categories, which is adopted by the Global Land Cover Characteristics (Loveland et al., 2000; Loveland & Belward, 1997) and MODIS land cover product (Justice et al., 1998). However, three modifications were made in order to meet our purpose of hydrological application. First, the agricultural area, just one category "Cropland" is defined in IGBP scheme, was divided to 5 sub-categories because agricultural fields play important role in water cycle in river basin, especially in the Yellow River basin where huge volume of water is used for irrigation. Second, mixed categories in IGBP scheme were excluded from our categories to keep the simplicity in our hydrological. Third, four categories were excluded in our classification because these categories exhibited similar characteristics in the current land surface features, and the feasibility study showed the difficulties in discrimination of these categories. Table 1 shows the land cover categories of this study and the correspondence to that of IGBP.

Table 1
Land cover categories with corresponding to IGBP categories.

IGBP land cover categories	The present study
Evergreen Needleleaf Forests	Evergreen Needleleaf Forests
Evergreen Broadleaf Forests	Evergreen Broadleaf Forests
Deciduous Needleleaf Forests	Deciduous Needleleaf Forests
Deciduous Broadleaf Forests	Deciduous Broadleaf Forests
Mixed Forests	-----
Closed Shrublands	-----
Open Shrublands	Open Shrublands
Woody Savannas	-----
Savannas	-----
Grasslands	Grasslands
Permanent Wetlands	-----
Croplands	Croplands (including paddy)
Croplands	Croplands (non-paddy)
Croplands	Double-cropping Fields (including paddy)
Croplands	Double-cropping Fields (non-paddy)
Croplands	Irrigated Fields
Urban and Built-up Lands	Urban and Built-up Lands
Cropland/Natural Vegetation Mosaics	-----
Snow and Ice	Snow and Ice
Barren	Barren
Water Bodies	Water Bodies

2.4 Classification method

The classification based on the decision tree method by means of land surface features described above was adopted due to the following advantages: (1) it is easy to customize the classification structure (shape of tree) by arranging the module which consist of input data and decision criteria, (2) it can control the classification result explicitly and easily by adjusting the threshold used in criteria, (3) it is robust to the noises in input data such as clouds if the noises were outside of the scope of decision module, and (4) it is capable to derive the stable classification result for another year due to the stability of the input data.

2.4.1 Pre-processing

Since MOD09Q1 product is one of the land product, no data are included over the deep ocean, furthermore, the pixels around the border of deep ocean are subject to have higher reflectance which is believed to be clouds or sea ices. Therefore, deep ocean and its border (4 pixels) were masked using image handling software and categorized to Water Bodies.

2.4.2 Decision tree classification

Fig. 1 shows the processing flow of the classification method and criteria used in each decision steps. Snow and Ice category is extracted in decision 1 using Sum_Day_Snow data. Erroneous pixels are excluded in decision 2. The main reason of the error is that at least one of land surface features could not be derived due to the cloud or snow. Water Bodies are discriminated using Ann_Min_Ref2 with the general characteristics that reflectance of water is much lower than that of land surface in near infrared wavelength. However, Ann_Min_Ref2 shows relatively higher reflectance near river mouth of large rivers as Chang Jiang River and the Yellow River. Therefore, another criterion based on Ann_Min_NDVI was added in order to avoid the misclassification of water to the land over these region. Since land surface except permanent snow and ice regions will pass through the previous decision steps, the following decisions are applied to the land area. Urban and Built-up Lands is generally difficult to discriminate from non and low vegetated area since these shows the similar features both in reflectances and NDVI. Therefore Hum_Set_DMSP was added as the criterion, and pixel with lower Ann_Max_NDVI and higher Hum_Set_DMSP is classified to Urban and Built-up Lands. Barren and Open Shrublands, where the vegetation coverage is constrained by climatic, geologic, or other various conditions, are extracted by means of Ann_Max_NDVI, which shows the most active status of vegetation in the year. Ann_Ave_Ref1 is applied in order to discriminate the herbaceous type and tree type vegetation in decision 7 on the basis that the tree

type vegetation shows generally darker reflectance in visible wavelength compared to herbaceous type vegetation.

The herbaceous type vegetations are classified to grassland or five kinds of agricultural fields. Double-cropping Fields are extracted in decision 8 by means of simultaneous use of Apr_Ave_NDVI and Jun_Ave_NDVI . The first cropping season is from February to May, and second season is from July to middle of November in this region, that is, NDVI in June is lower than that of April in this region. This characteristics is quite unique from the phenological and hydrological point of view, compared to natural grasslands or single cropping agricultural lands. The pixel is consequently labeled as paddy or non-paddy in decision 13 according to the Ann_Min_Ref1 criterion. The three criteria used for Irrigated Fields in decision 9 were derived fully empirically by investigation of the feature images. Passed pixels will be classified to Croplands or Grasslands according to Ann_Max_Ref1 criterion. If the reflectance in visible wavelength is lower than the threshold, the pixel is categorized to the Croplands, and higher is to Grasslands. This criterion is also derived empirically based on the rough assumption that agricultural field has darker reflectance in several periods of year than natural grassland. The pixel categorized in Croplands are labeled as paddy and non-paddy by same criterion applied to the Double-cropping Fields.

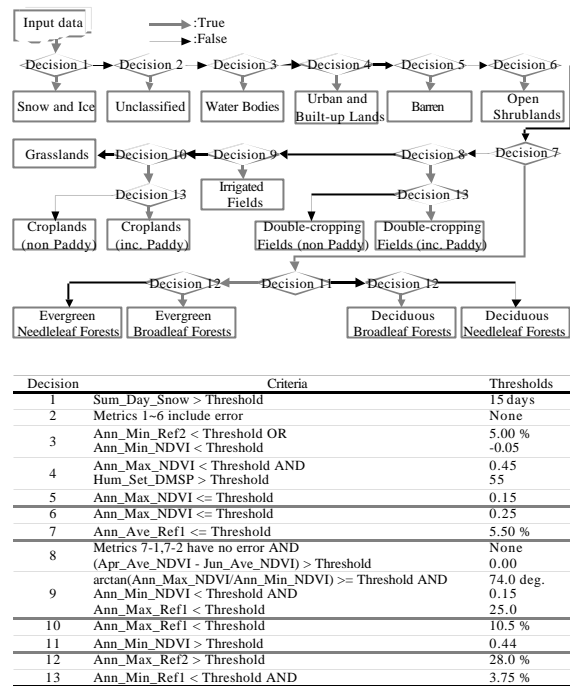


Fig. 1 Flowchart of decision tree classification and criteria in each decision step.

The tree type pixels are classified to four forest categories, "Evergreen Needleleaf Forests", "Evergreen Broadleaf Forests", "Deciduous Needleleaf Forests", and "Deciduous Broadleaf Forests", according to the seasonality and leaf type. Seasonality is determined by Ann_Min_NDVI criterion, which shows the least active status of vegetation in the year. Leaf type is measured by Ann_Max_Ref2 , that is, brighter forest in near infrared wave region is classified to broadleaf, and darker is to needleleaf.

The determination of the thresholds is critical issue with regard to the classification accuracy, since it directly controls the classification result. We decided the each thresholds by means of following two methods. MODIS land cover product (abbreviated as MOD12Q1) was used as the training data for

decisions 3, 5, 6, 7, 11 and 12 as first method. Individual land surface features were sampled every four pixels in order to overlay to MOD12Q1, and training data were extracted by each land cover area in MOD12Q1. The thresholds were derived from the comparison of pixel based histograms of each category. Another method was simple visual interpretations. The thresholds in decision 1, 4, 8, 9, 10, and 13 were derived manually with reference to existing land cover maps using commercial image handling software.

2.5 Accuracy assessment

The classification result was compared to two types of reference data with Chinese province base.

One reference is existing digital land cover map, "1 km land-use & land cover raster data of China (abbr. as CASW data)" provided by CASW Data Technology Co., Ltd. (<http://www.casw.com.cn/>). Land cover percentage of 25 land cover type within 1 km grids in 1996 are derived from Landsat images. This data was geometrically re-projected to the same projection as our land cover classification map in the resolution of 30 arc seconds, thereafter, the pixel are aggregated to the province using province boundary data. The land cover categories in both classification map were aggregated to 6 general categories (forest, agricultural land, grassland, barren, paddy field, and dry field) as following:

The present study:

Forest; Evergreen Needleleaf Forests, Evergreen

Broadleaf Forests, Deciduous Needleleaf Forests, and Deciduous Broadleaf Forests
 Agricultural field; Croplands (inc. paddy), Croplands (non-paddy), Double-cropping Fields (inc. paddy), Double-cropping fields (non-paddy), and Irrigated Fields
 Grassland; Grasslands
 Barren; Barren
 Paddy field; Croplands (inc. paddy) and Double-cropping fields (inc. paddy)
 Dry field; Croplands (non-paddy), Double-cropping fields (non-paddy), and Irrigated Fields

CASW data:

Forest; woodland, sparse woodland, and other woodland
 Agricultural field; dry land and paddy field
 Grassland; low-, medium-, and hi-covered grassland
 Barren; gobi desert, barren land, barren rock, and sand ground
 Paddy field; paddy field
 Dry field; dry land

Another reference is Chinese census data. Province based land cover area of aggregated four categories (forest, agricultural field, paddy field, and irrigated field) are compared to two kinds of census data. Forest area is obtained by counting the area of needleleaf forest, broadleaf forest, commercial forest, and bamboo grove in the 4th Chinese census of forest resources (1989~1993) derived from Chinese Forest Science Data Center website (<http://www.cfsdc.org/>). Agricultural field, paddy field and irrigated field were based on the

total planted area, paddy area, and effective irrigated area in 2000, respectively, derived from National Bureau of Statistics of China website (<http://www.stats.gov.cn/>). Area of forest, agricultural field, and paddy field of the classification are same as aggregated categories in previous comparison with existing land cover map. Irrigated field is total area of Croplands (inc. paddy), Double-cropping Fields (inc. paddy), and Irrigated Fields. Five provinces, Heilongjiang, Inner Mongolia, Tibet, Xinjiang, and Hainan were excluded from the comparison, since our classification map do not cover the whole area of these provinces.

3. Results and discussion

3.1 Classification result

Fig. 2 shows the classification result. Clear zonal distribution of Barren, Open Shrublands, Grasslands, Croplands, and Forests appeared from the inner continent up to Pacific Ocean. Barren correspond to Gobi and Taklamakan Desert. Open Shrublands was found in transition zone of barren and grassland. This category was sensitive to the threshold value, and boundary changed significantly by the threshold value of Ann_Max_NDVI. It is inferred that inter-annual variation is also large in this region since vegetation in semi-arid region is sensitive to climate condition. Grasslands spread in Mongolia, Russia, and north eastern to south western China, surrounding the open shrublands. Forests were distributed in most outer zone mainly near Pacific Ocean: northern Mongolia, eastern Siberia, Korean Peninsula, Japan, southern China, and South East Asian countries to India. Evergreen

forests were dominated by broadleaf forest rather than needleleaf forest. Evergreen Broadleaf Forests were found in tropical to subtropical zone, subarctic zone, and Japan. Evergreen Needleleaf Forests were found in mountainous zone such as Himalaya Mountains and Sikhote Alin Mountains in eastern Russia. Deciduous Broadleaf Forests are distributed in Gansu, Sichuan, and Hunan provinces in China, where the northern boarder of subtropic evergreen forests, and also distributed in north eastern China around Liaoning and Jilin provinces, and Korean Peninsula where the southern border of subarctic evergreen forests. Five kinds of Croplands were widespread between grassland and forest filling the gap of intricately distributed forests. Paddy fields indicators were appeared dominantly South to South Eastern Asian countries, southern China, and North Eastern China Plain. Double-cropping Fields, which consist both of paddy and non-paddy fields, were found in downstream including the North China Plain and Wei Basin in Shaanxi province where one of the branch of the Yellow River, Wei River flows. A number of large irrigated districts including two huge districts of Ningxia and Hetao were extracted in upstream of the Yellow River. The distribution of irrigated and double cropping fields showed better agreement with Chinese irrigation map (Prof. Jianyao Chen, personal communication) shown in Fig. 3, even though the irrigation map indicates just the Yellow River basin and irrigated area in mid and downstream was categorized in Double-cropping Fields in our classification. Unclassified data, which were mainly due to the cloud, clustered around Himalaya Mountains where it could be

frequently cloudy or cloud detection algorithm

seems to confuse the cloud with the snow.

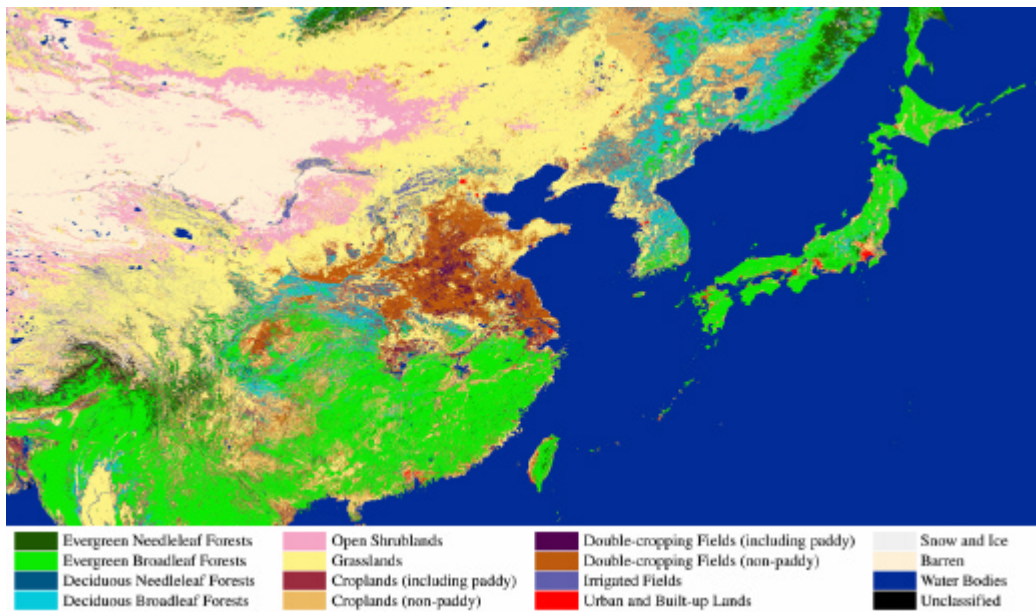


Fig. 2 Land cover classification result

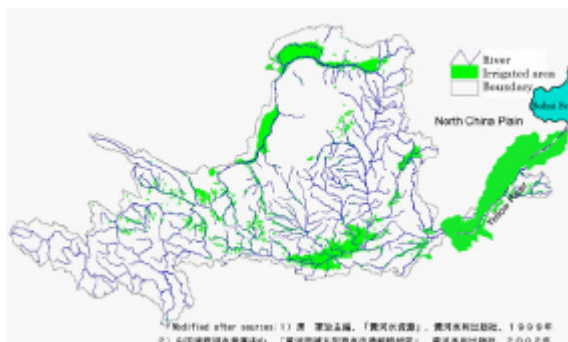


Fig. 3 Irrigation map of the Yellow River basin (Prof. J. Chen, personal communication).

3.2 Comparison with Chinese land cover map

Fig. 4 shows the Chinese province map, and Fig. 5 shows the scatter diagrams of land cover area by Chinese provinces. Unfortunately no information was obtained about the accuracy of CASW data.



Fig. 4 Chinese province map.

The comparison showed the good agreements in Forest, Agricultural Field, Grassland, and Barren, but low agreements two agricultural sub-categories, Paddy field and Dry field. The strong geographical dimensions were found in all the categories. Forest area was underestimated in north eastern provinces (Inner Mongolia, Liaoning, Heilongjiang, and Jilin) but overestimated in south eastern provinces (Sichuan, Hunan, Fujian, and Jiangxi). Agricultural field was underestimated in north eastern provinces (Inner Mongolia, Liaoning, and Jilin) but

overestimated in south western provinces (Qinghai, Guizhou, Yunnan, and Tibet). Grassland was underestimated in western provinces (Qinghai, Inner Mongolia, Xinjiang, and Tibet) but overestimated in north eastern provinces (Heilongjiang, Jilin, Liaoning, and Hebei). Barren was underestimated in south western to central provinces (Tibet, Sichuan, Shaanxi, and Yunnan) but overestimated in western provinces (Inner Mongolia, Qinghai, Xinjiang, and Gansu). Paddy field was underestimated in central to eastern provinces (Hunan, Jiangxi, Anhui, Jiangsu, and Guangdong) but overestimated in north eastern provinces (Heilongjiang and Inner Mongolia) and Yunnan province, provinces with larger paddy field were generally underestimated and vice versa. Dry field was underestimated in northern to eastern provinces (Inner Mongolia, Jilin, Gansu, and Shandong) but overestimated in southern provinces (Tibet, Guangxi, and Yunnan).

From geographical viewpoint, north eastern provinces showed the underestimation in forest, agricultural field and dry field, but overestimation in paddy and grassland. Central to eastern provinces where the forest was overestimated showed the underestimation in paddy fields. The province where grassland was underestimated exactly corresponded the overestimated provinces in barren, and these provinces have larger area both of grassland and barren. Geographical distribution in these provinces showed the clear zonal distribution of Barren, Open Shrublands, and Grasslands in our classification. The discriminations of these three categories resulted in overestimation in barren and underestimation in grassland.

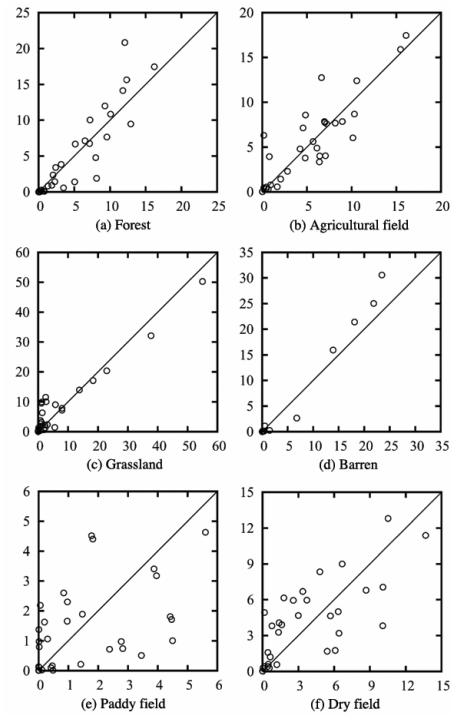


Fig. 5 Comparison of classification result with CASW data. Horizontal axis is land cover area of Chinese provinces in 10000 km² derived from CASW data and vertical axis is same but derived from classification.

3.3 Comparison with Chinese census

Fig. 6 shows the scatter diagrams of land cover area in each Chinese provinces derived from ground based census and our classification.

Forest and agricultural field showed less agreements relative to previous comparison with land cover map. Our classification overestimated nearly double of census data in forest and agricultural field, even though the geographical dimensions were similar. Other studies also resulted in the overestimation of classification based land cover area for forest (Hansen et al., 2000), and for agricultural and irrigated area (Frolking et al., 1999). The comparison of land cover area between classification and ground

based or registration based census, which is appropriate to be called as "land use" rather than "land cover", is complicated due to the difference in recognition of the land surface. Furthermore, coarse resolution data generate the mixture of land cover in one pixel especially in the heterogeneous land cover. Several kinds of land cover as farm roads and open spaces relevant to agricultural field are included in one pixel with the spatial resolution of 7.5 arc seconds, even it is classified as agricultural field.

The area of paddy field in two reference data were less consistent, and area in census was smaller than that in existing land cover map, this was also pointed out by Frohling et al. (2002). However, the geographical dimension was similar in both comparison i.e. central to eastern provinces showed the underestimation, and north eastern provinces showed the overestimation.

The irrigated area is underestimated in the North China Plain such as Shandong, Hebei, Jiangsu, and Hunan province. This underestimation was due to the discrimination of paddy field from double-cropping field. The overestimated provinces were Qinghai, Shanxi, Sichuan, Yunnan, etc. The extraction of Irrigated Fields category caused the overestimation in former two provinces, and discrimination of paddy fields from cropland in latter two provinces.

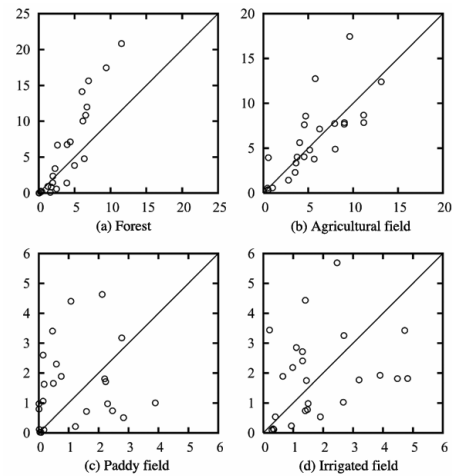


Fig. 6 Comparison of classification result with Chinese census. Horizontal axis is land cover area of Chinese provinces in 10000 km² derived from census and vertical axis is same but derived from classification.

4. Conclusions

Land cover classification map for East Asia region in 2000 was produced by means of two kinds of MODIS land products and one OLS product in order to be applied to a hydrological model. The classification method was based on the simple decision tree method using eleven land surface feature images which represent the spectral and phenological characteristics of land surface. The decision tree method is so flexible that we can develop the purpose-designed classification tree by arranging the modules which consist of input images and decision criteria. Additionally, It is robust for the local noises due to clouds or snows, if the noise arises at the out of classification interest. We used the two kinds of MODIS land products, Surface Reflectance 8-Day L3 Global 250m SIN Grid (MOD09Q1) and Snow Cover 8Day L3 Global 500m SIN Grid (MOD10A2), as input data because their high spatial resolutions are suitable for East Asia where

the land surface is much heterogeneous composed of small land cover units. We selected the fifteen land cover categories, ten of them were acceded to the IGBP classification scheme and other five agricultural categories: croplands (including paddy), croplands (non-paddy), double-cropping fields (inc. paddy), double-cropping agricultural field (non-paddy) and irrigated fields were selected because of their hydrological importance. The thresholds in the classification process are essential factors to control the classification result. We used the MODIS land cover product and existing land cover maps for determining the thresholds owing to the restricted availability of training data. The comparison of the aggregated six categories with existing Chinese land cover map showed the good agreements in forest, agricultural field, grassland, and barren categories, but low agreements in agricultural sub-categories, paddy fields and dry fields. The another comparison of forest, agricultural field, paddy field, and irrigated fields with Chinese province based census indicated the overestimation in forest and agricultural field, and poor correlation in paddy field and irrigated field. Accuracy assessment of the classification result is complicated task by reason of absence of proper references. The comparison between classification maps or ground based survey is affected to some extent by the incidental factors as spatial resolutions, data source, and the name and definition of the category, rather than classification itself. Nevertheless, the comparison is useful for the improvement in the method and parameters, and it shows us the way to the most reasonable result. The acquisition of effective

input data in discriminating the land cover type and adjustment of the thresholds by means of ancillary information as high resolution satellite image are required for further progress in this study.

Acknowledgments

This study was carried out as part of Research Revolution 2002 project supported by Ministry of Education, Culture, Sports, Science and Technology (MEXT) in Japan. We are grateful to Dr. Xieyao Ma and Prof. Jianyao Chen for providing helpful information about land cover and hydrological situation in China. We also would like to thank Dr. Keisuke Hoshikawa for processing the several digital maps used in this study.

References

- Frolking, S., Xiao, X., Zhuang, Y., Salas, W., & Li, C. (1999). Agricultural land-use in China: a comparison of area estimates from ground-based census and satellite-borne remote sensing. *Global Ecology and Biogeography*, 8, 407-416.
- Frolking, S., Qiu, J., Boles, S., Xiao, X., Liu, J., Zhuang, Y., Li, C., & Qin X. (2002). Combining remote sensing and ground census data to develop new maps of the distribution of rice agriculture in China. *Global Biogeochemical Cycles*, 16(4), 1091-1100.
- Hansen, M. C., Defries, R. S., Townshend, J. R. G., & Sohlberg, R. (2000). Global land cover classification at 1 km spatial resolution using a classification tree approach. *International Journal of Remote Sensing*, 21(6/7), 1331-1364.
- Justice, C. O., Vermote, E., Townshend, J. P. G., Defries, D., Roy, D. P., Hall, D. K., Salomonsen, V. V., Privette, J. L.,

- Riggs, G., Strahler, A., Lucht, W., Myneni, R. B., Knyazikhin, Y., Running, S. W., Nemani, R. R., Wan, Z., Huete, A. R., Leeuwen, W. V., Wolfe, R. E., Giglio, L., Muler, J. P., Lewis, P., & Barnsley, M. J. (1998). The Moderate Resolution Imaging Spectroradiometer (MODIS): land remote sensing for global change research. *IEEE Transactions on Geoscience and Remote Sensing*, *36*(4), 1228-1249.
- Loveland, T. R., & Belward, A. S. (1997). The IGBP-DIS global 1 km land cover data set, DISCover: first results. *International Journal of Remote Sensing*, *18*(15), 3289-3295.
- Loveland, T. R., Reed, B. C., Brown, J. F., Ohlen, D. O., Zhu, J., Yang, L., & Merchant, J. W. (2000). Development of a global land cover characteristics database and IGBP DISCover from 1-km AVHRR Data. *International Journal of Remote Sensing*, *21*(6/7), 1303-1330.
- Ma, X., Hiyama, T., Fukushima, Y., Hashimoto, T. (1998). A numerical model of the heat transfer for permafrost regions. *Journal of Japan Society of Hydrology and Water Resources*, *11*(4), 346-359.
- Ma, X., Fukushima, Y., Hiyama, T., Hashimoto, T., & Ohata, T. (2000). A macro-scale hydrological analysis of the Lena River basin. *Hydrological Processes*, *14*, 639-651.
- Ma, X., & Fukushima, Y. (2002). A numerical model of the river freezing processes and its application to the Lena River. *Hydrological Processes*, *16*, 2131-2140.
- Salomonson, V. V., Barnes, W. L., Maymon, P. W., Montgomery, H. E., & Ostraw, H. (1989). MODIS: advanced facility instrument for studies of the Earth as a system. *IEEE Transactions on Geoscience and Remote Sensing*, *27*(2), 145-153.

V List of related meetings

(1) **Global Water System Project (GWSP) - Asia Meeting**

August, 2005, Kyoto, Japan (tentative)

Organizers: RIHN and GWSP

Yoshihiro Fukushima, Project Leader

Makoto Taniguchi, Secretary General

Research Institute for Humanity and Nature (RIHN),

Inter-University Research Institute Corporation, National Institutes for the Humanities

335 Takashima-cho, Kamigyo-ku, Kyoto 602-0878, Japan

Tel: +81-75-229-, Fax: +81-75-229-6150

E-mail: YRiS@chikyu.ac.jp, URL: http://www.chikyu.ac.jp/index_e.html